ELSEVIER

Catalysis Today 61 (2000) 55–64

CATALYSIS TODAY

www.elsevier.com/locate/cattod

Syngas formation by direct oxidation of methane Reaction mechanisms and new reactor concepts

G. Veser*,[1], J. Frauhammer, U. Friedle

Institut für Chemische Verfahrenstechnik, Universität Stuttgart, Böblinger Strasse 72, 70199 Stuttgart, Germany

Abstract

The reaction mechanism of direct catalytic oxidation of methane to syngas over a platinum catalyst under high temperature, short contact time conditions was studied with a detailed reactor and reaction model. Based on a detailed analysis of this mechanism, new integrated reactor concepts were deduced. Two concepts were studied in detail: a fixed bed reactor with integrated recuperative heat exchange, and a catalytic membrane reactor with distributed reactant feed. The reactor concepts are presented, and advantages and problems of the concepts are discussed.

Keywords: Methane oxidation; Platinum catalyst; Synthesis gas; Integrated reactor concepts

1. Introduction

Multifunctional or integrated reactor concepts are currently the focus of intense research in reactor engineering. In these concepts, different unit operations such as heat exchange, distributed feed supply, or product separation are integrated in addition to the chemical reaction into one multifunctional apparatus. Much studied examples of such new reactor concepts are countercurrent reactors and membrane reactors. The aim of the countercurrent reactor concept is to affect the reactor temperatures through an internal heat exchange, while membrane reactors are typically used to selectively separate one or more reactants from the reacting mixture to influence reaction selectivities and conversions.

The direct coupling of these different unit operations, however, leads to a considerably higher degree of complexity in these reactor concepts. While the general behaviour of the reactor can often still be understood in terms of simplified models, an optimised reactor design now usually requires a rather detailed understanding of the particular reaction system. In the present paper we will illustrate this using the example of syngas production through direct catalytic oxidation of methane, for which two promising multifunctional reactor concepts could be deduced based on a detailed analysis of the surface reaction mechanism.

The direct catalytic oxidation of methane to syngas is an interesting alternative to the conventional steam reforming [1–4]. The process can be conducted autothermally at high reaction temperatures and very short contact times which allow for very high reactor throughputs and a compact reactor size. Particularly, noble metal coated monolith reactors have shown good syngas selectivities and yields [5]. In previous studies we developed a detailed elementary step reaction model for syngas formation over Pt-coated monoliths which was verified against experimental results. A good agreement between model results and experimental data was found, indicating that the model

* Corresponding author. Fax: +49-208-306-2995.
E-mail address: veser@mpi-muehlheim.mpg.de (G. Veser).
[1] Max-Planck-Institut Für Kohlenforschung Kaiser-Wilhelm-Platz 1, 45470 Mülheim/Ruhr, Germany.

0920-5861/00/$ – see front matter
PII: S0920-5861(00)00378-3

describes the essential reaction steps well [1]. Based on a detailed analysis of this surface reaction mechanism, essential steps in the reaction mechanism could now be identified. This not only leads to a better fundamental understanding of this important reaction, but also allows us to deduce new and optimised reactor concepts for this system. We see this step as a promising connection between two different basic research areas: the fundamental modelling of catalytic surface reactions based on elementary step mechanisms and the development of novel reaction engineering concepts.

In the following, the reaction mechanism will be briefly laid out, the multifunctional reactor concepts for the catalytic oxidation of methane will be presented and hurdles on the way to a technical application of these concepts will be discussed.

2. Reactor and reaction model

The basic reactor and reaction model for the Pt monolith reactor has been presented in detail in a separate paper [6]. However, since this model forms the basis for the extended reactor models on which the discussion of the new reactor concepts is based in this paper, a brief description is given in the following.

The reactor model is a one-dimensional two-phase dispersion model which contains detailed one-dimensional mass and energy balances for the gas phase and the catalytic monolith. Two major simplifying assumptions were made in the derivation: the reaction is assumed to proceed predominantly on the catalyst surface, and mass transfer limitations in the boundary layer above the catalyst are neglected. Both assumptions have been verified in previous studies [1,6].

The mass balance equation for the gas phase comprises mass transport by convection and dispersion as well as adsorption and desorption from the catalyst surface. The energy balance for the gas phase comprises heat transport and dispersion, while the energy balance for the catalytic monolith contains heat transport by conduction and the heat release by the surface reaction. The two phases are thermally coupled through convective heat transfer between the gas and the catalyst. The reactor parameters in the simulations were taken from the steady-state experiments by Hickman and Schmidt [2].

The surface reaction mechanism constitutes a detailed elementary step mechanism which comprises balance equations for CH_4, C, CO, CO_2, O, H, OH, and H_2O on the catalyst surface. The mechanism thus describes all possible surface reaction intermediates for the considered partial and total oxidation routes with the exception of the intermediate species CH_3, CH_2 and CH during methane decomposition since no experimental data is available for these intermediate steps. Therefore, a single, irreversible reaction step according to $CH_{4,ad} + 4S \rightarrow C_{ad} + 4H_{ad}$ is assumed for methane decomposition. O_2 and H_2 adsorption are assumed to be dissociative and all adsorption steps are taken to be non-activated and follow kinetic gas theory. Activation energies and sticking coefficients in the model were taken from experimental investigations in the literature wherever possible.

The described system of balance equations forms a system of coupled parabolic differential equations which are solved numerically using the fully adaptive method-of-lines (MOL) algorithm PDEXPACK [7]. The full spatial and temporal adaptivity of the algorithm is based upon the relative errors for time and space discretizations for every state variable at every gridpoint and every time step. This procedure allows for a reliable integration of the very stiff system and an accurate resolution of the very steep gradients observed during typical high temperature catalytic oxidation reactions.

3. Reaction mechanism

Detailed simulation studies with the above described model demonstrate the importance of high reaction temperatures for this reaction system. As shown in Fig. 1, both methane conversion and syngas selectivities increase steeply with increasing pre-heat of the feed gases. Interestingly, while conversions and selectivities are strongly influenced by the increasing pre-heat, reaction temperatures increase much less pronouncedly (not shown in the graph). Instead, the increasing feed gas temperature increases syngas selectivities so strongly that the heat release by the reaction effectively drops despite increasing conversions, and thus the overall temperature remains almost unchanged. Obviously, the reaction is quite efficient in turning thermal energy into chemical energy.

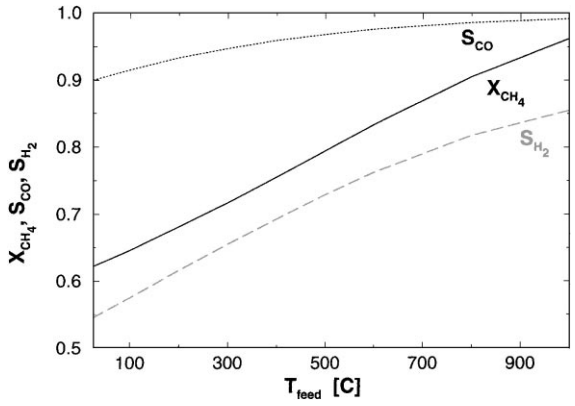

Fig. 1. Effect of increasing pre-heat on methane conversion and syngas selectivities in partial methane oxidation over Pt. The simulation results for the steady state of the reactor with $CH_4/O_2 = 1.6$ and $N_2/O_2 = 4$ (air) are shown. Oxygen conversion was complete for all conditions shown.

Furthermore, the simulation studies indicate that catalytic methane oxidation under fuel rich high-temperature conditions proceeds predominantly via a direct oxidation mechanism. There has been much discussion and much confusion about this, mostly based on the experimental observation that in TAP reactor and other ignition-type experiments there is always a strong CO_2 and H_2O pulse preceding the partial oxidation products. This seems to indicate that the reaction is actually proceeding via an indirect reaction mechanism in which part of the methane is initially being combusted to CO_2 and water, and the remaining methane is then being converted by steam reforming and/or CO_2 reforming to give the eventual products CO and H_2.

This strong initial total oxidation pulse is reproduced in our simulation studies as shown in the left-hand side graph in Fig. 2. However, the reason for this reaction behaviour is *not* based on a sequential reaction mechanism, but rather on the adsorption characteristics of the main reactants CH_4 and O_2. Since the sticking coefficient of O_2 is considerably higher than the hydrocarbon, O_2 is preferentially adsorbed on the catalyst surface. This leads to an "over-oxidized" surface state before ignition of the reaction, i.e. the catalyst surface is predominantly oxygen covered (see Fig. 2, right-hand side graph). Upon ignition, this adlayer is reacted off. During this process, the CH_4:O_2 ratio on the surface is initially

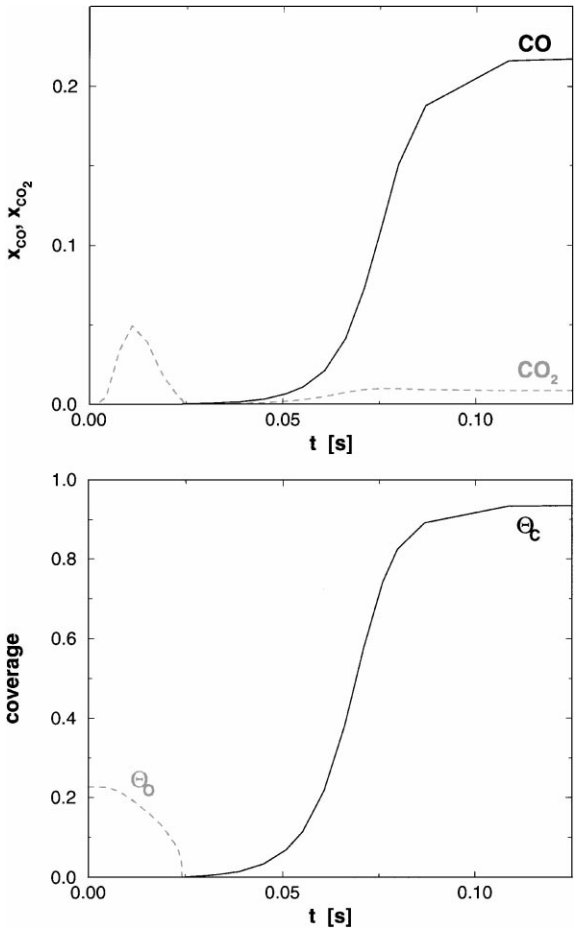

Fig. 2. Ignition in CH_4 oxidation over Pt: CO and CO_2 molar fractions in the gas phase (left graph) as well as oxygen and carbon coverage (right graph) at the reactor exit. A sequence from CO_2 to CO and, in parallel, from θ_O to θ_C can be seen. The simulation results for the ignition upon introducing a methane/air mixture with $CH_4/O_2 = 1.6$ and $T = 1200°C$ into a reactor initially filled with air are shown.

very low (i.e. the *catalytic* reaction conditions are actually very fuel *lean*) therefore leading to total combustion of the hydrocarbon. After this ignition pulse, however, a rather high carbon coverage builds up on the surface and the reaction proceeds very selectively towards the partial oxidation products.

The temporal succession during the ignition process is also reflected in the spatial reactor profiles at steady state, shown in Fig. 3. Again the reason for this transition from total oxidation products (CO_2 and H_2O) to partial oxidation products (CO and H_2) can

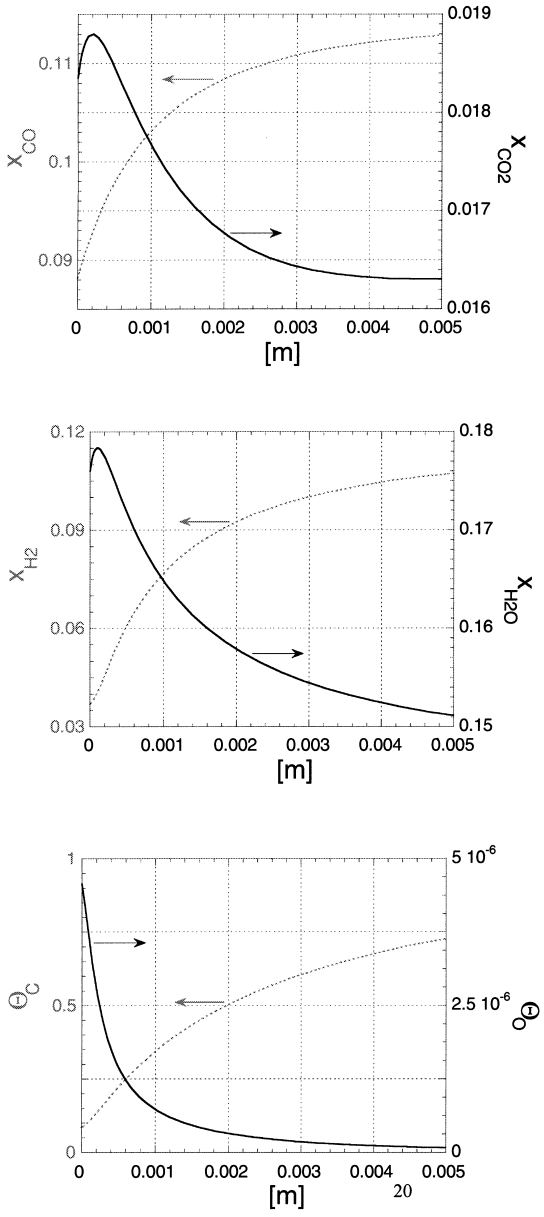

Fig. 3. Spatial profiles of the molar fractions of CO_2 and CO (left), H_2O and H_2 (middle), and oxygen and carbon coverages (right) along the reactor axis at steady state. Conditions were: $CH_4/O_2 = 1.6$, $N_2/O_2 = 4$, $T_{in} = 25^{\circ}C$.

be found in the preferential oxygen adsorption, which leads to a rather lean reaction mixture on the catalyst surface and thus to total oxidation of some of the inlet methane. During this total oxidation phase, more oxygen is consumed than methane (due to the stoichiometry of the total oxidation reaction) and therefore the methane-to-oxygen ratio in the gas phase increases. As soon as the oxygen partial pressure has dropped low enough to compensate for the difference in sticking coefficients, the reaction conditions on the catalyst shift to "truly" fuel lean conditions and the reaction pathway switches to selective partial oxidation.

The much steeper maximum in the H_2O molar fractions in comparison to that in the CO_2 molar fractions already indicates, however, that it is not only the transition from fuel lean to fuel rich surface conditions that causes the rise in the H_2 molar fraction, but rather hints at the importance of secondary steam reforming reactions in the current system. While we find that steam reforming does occur in this system, a reaction path analysis shows that no more than about 25% of the H_2 formed in this reaction stems from a steam reforming path. Clearly, direct oxidation is the primary reaction path for the formation of both H_2 and CO.

Finally, a remarkable difference in the apparent ignition mechanisms between the catalytic reaction and homogeneous hydrocarbon oxidation reaction should be pointed out: while the reactants and intermediates during homogeneous hydrocarbon oxidation typically undergo a succession of increasingly 'deep' oxidation steps [8], i.e. while for homogeneous reactions in the gas phase the partial oxidation product is typically an intermediate in the reaction path to the total oxidation product, the *exact opposite* appears to be true for the catalytic reaction when looking at the sequence of reaction products in the gas phase. This becomes obvious when comparing the results of a simple PFR reactor simulation using a detailed purely homogeneous methane oxidation mechanism (GRI Mech 2.11, [9], see Fig. 4) with the results of the catalytic reaction mechanism in Fig. 3. However, while the succession in the homogeneous reaction products is due to a sequential reaction scheme, this is *not* true for the heterogeneous catalytic reaction. Rather, the "over-oxidised" initial state of the catalyst is first reduced to its steady state coverage by a transient total oxidation wave that gives rise to a total oxidation product pulse at the reactor exit.

This observation has important consequences for the understanding and evaluation of transient kinetic experiments — such as in TAP-reactors — during catalytic hydrocarbon oxidation over platinum. In those types of experiments, the repetitive pulsing of

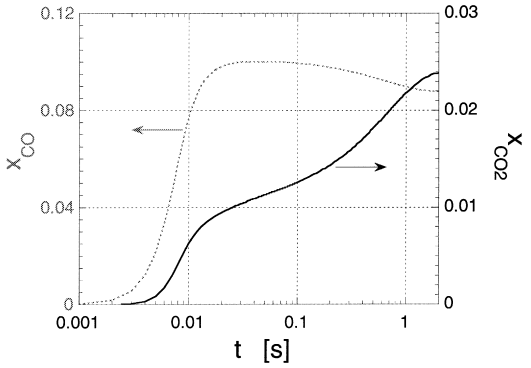

Fig. 4. Succession of CO and CO_2 in a purely homogenous reaction scheme of methane oxidation with air (conditions were: $CH_4/O_2 = 1.6$, $T = 1200°C$). In contrast to the catalytic reaction mechanism (Fig. 2), the homogeneous oxidation pathway follows a succession from partial to total oxidation.

reactants will force the catalyst surface to undergo periodic oxidation and reduction cycles, in which each new hydrocarbon pulse will again lead to a succession of total oxidation to partial oxidation products. If the *spatial* dynamics of the reactor system are not taken into account, this will lead to a misinterpretation of the experimental observations in terms of *temporally* sequential steps in the reaction mechanism, which then could be taken to indicate an indirect oxidation route as the primary reaction path in these reaction systems.

4. Reactor concepts

The simulation studies regarding the reaction mechanism lead to two quite obvious conclusions: firstly, as high reaction temperatures as possible seem necessary to optimise reaction selectivities and conversions. While this can be done by externally heating the reactor or pre-heating the feed-gases as shown in Fig. 1, this would be a rather expensive and unsophisticated way of achieving the desired effect. Therefore, we devised an integrated reactor concept, in which the sensible heat of the hot reaction products is used to pre-heat the feed gases internally. This concept will be discussed in the following paragraph.

A second reactor concept, focuses on a kinetic rather than a thermal optimisation of the reactor: clearly, the strong oxygen adsorption on the catalyst surface leads to a loss in reaction selectivity due to the above discussed total oxidation zone at the reactor entrance. Therefore, a reduction of the oxygen partial pressure in this area by distributing the oxygen feed along the reactor axis seems a viable way to improve selectivities in the current system. This concept will be discussed further in Section 4.2.

4.1. Heat integration

Based on the above considerations, we designed and tested a reactor with an internal heat recuperation, by reversing the flow direction of the hot effluent gases from the reaction zone and thus pre-heating the feed gases through an internal countercurrent heat exchanger [10]. In addition to the heat exchange, particular care was taken with respect to reactor safety, since potentially explosive mixtures of methane and air had to be handled at elevated temperatures. Therefore, the gases were fed separately into the reactor and were only pre-mixed right in front of the reaction zone by injecting the inner feed (F1) into the outer feed (F2) stream (see Fig. 5). Static mixers additionally ensured a well mixed gas stream at the catalyst entrance. As a final safety measure, the reactor is closed up at its hot end by a rupture disk which should lead to a benign release of a pressure wave in case of an explosion. The reactor design is shown schematically in Fig. 5.

Fig. 6 shows the performance of the laboratory reactor for the partial oxidation of methane with air over a Pt catalyst. Obviously, a good heat integration into the

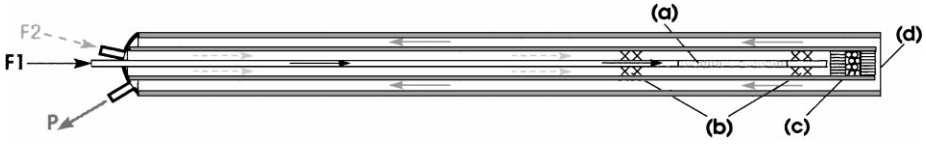

Fig. 5. Countercurrent heat-exchange reactor with separate feed of reactants (F1 and F2), pre-mixing zone (a), static mixers (b), catalytic reaction zone (c), and a rupture disk (d). The cold product gases leave the reactor through exit P.

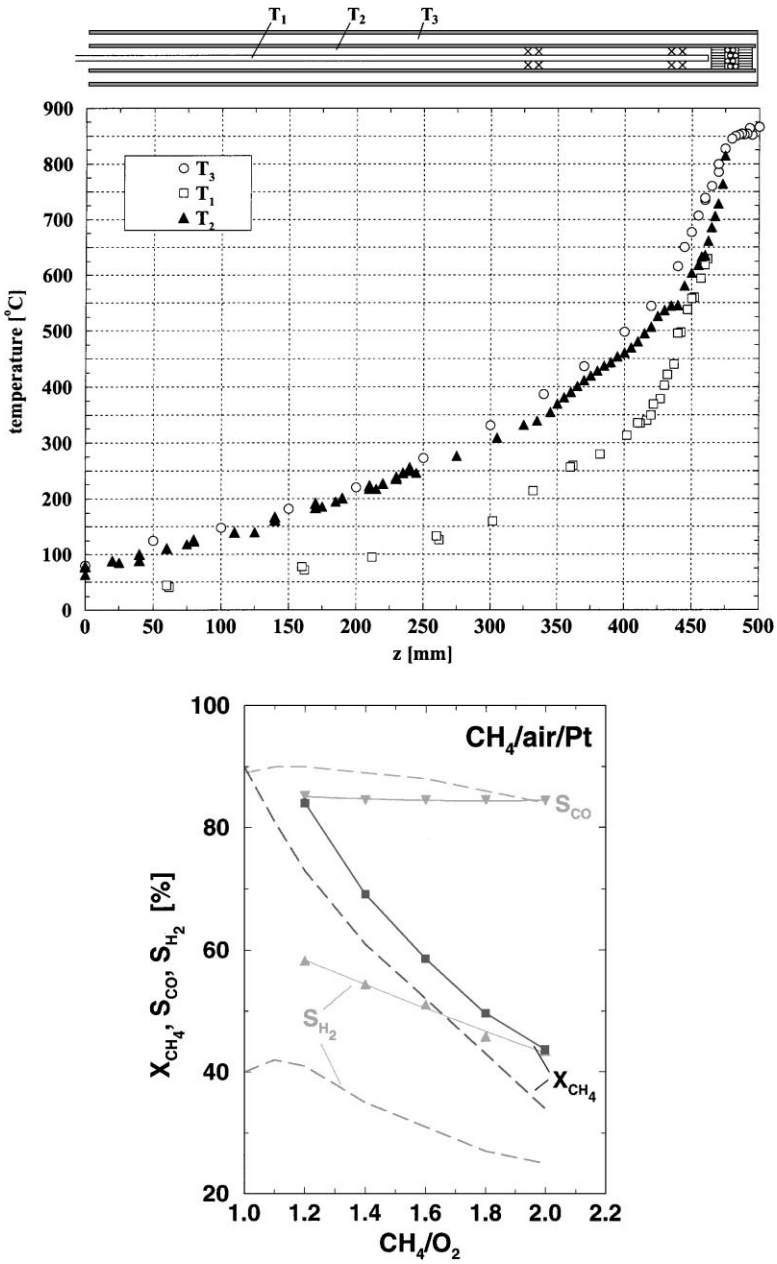

Fig. 6. Experimental results for the countercurrent heat-exchange reactor: shown are typical temperature profiles along the reactor axis (upper) as well as methane conversions and syngas selectivities for varying CH_4/O_2-ratios over Pt in comparison between a conventional fixed bed reactor (dashed lines) and the countercurrent heat-exchange reactor (symbols and full lines) at steady state. The data for the conventional fixed bed reactor is taken from the work of Hickman and Schmidt [5]. Conditions were: $N_2/O_2 = 4$ and $T_{in} = 25°C$.

reactor is achieved, reaching very high pre-heat temperatures ($T_2 > 800^\circ$C, left-hand side graph) right in front of the catalytic reaction zone, while effectively cooling down the exit gases to temperatures below 100°C and thus greatly facilitating downstream gas handling. Additionally, a considerable performance enhancement can be achieved with respect to reaction selectivities and conversions, as shown in the upper graph in Fig. 6. Methane conversions increase by about 10% (absolute percentage points) and hydrogen selectivities even by about 20%. Surprisingly, CO selectivities drop slightly, however, which we attribute to a catalytic blind activity of the highly alloyed stainless steel under the extreme high temperature reaction conditions (reactor temperatures are around 900–1100°C at the reactor head). Furthermore, an EDX analysis of the catalyst after prolonged reactor operation showed Fe depositions on the catalyst and the support, apparently from a reactive deterioration of the reactor steel housing. Thus, a more suitable reactor material (such as high-temperature ceramics) remains to be found.

Using the reactor and reaction model described in the previous section, we simulated the experimental behaviour of the reactor with integrated heat exchange, and found a very good agreement between experiment and simulation results (Fig. 7). This strengthens further the validity of our kinetic scheme, and helps to understand a few crucial points about the described reactor: first of all, we find in our simulations that about 50% of the heat generated in the reaction gets lost through the reactor head, i.e. through the very thin rupture disk against which the hot reaction gases impinge vertically before being reflected into the outer reactor (heat-exchange) tube. Obviously, there is a strong trade-off between reactor safety and performance: since the rupture disk is a redundant safety measure, the reactor performance could be further improved significantly by reducing the heat losses through a more substantial reactor enclosing.

Furthermore, the simulations help to explain the pronounced bend in the experimental temperature curves in Fig. 6: in the pre-mix area, the inner feed gases (F1) are injected into the outer feed gases (F2), leading to a strongly turbulent flow in this area and a correspondingly increased heat transfer coefficient. Taking this into account in our simulations, both the bend in the temperature profile of the feed gas side as well as the rapid convergence of the temperatures

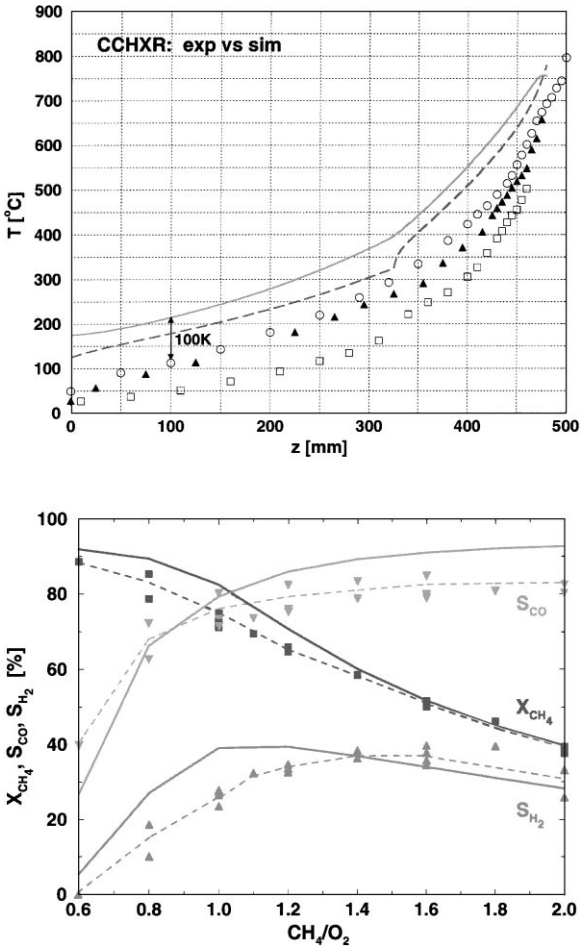

Fig. 7. Comparison between experiments and simulation results for the countercurrent heat-exchange reactor: Experimental (symbols, cp. Fig. 6) and calculated (lines) temperature profiles (upper) as well as methane conversions and syngas selectivities (symbols and dashed lines: experimental data; solid lines: simulation results) for varying CH_4:O_2 ratios. For better visibility, the calculated temperature profiles are offset by 100 K with respect to the experimentally measured profiles. The data were taken for a diluted reactant mixture ($N_2/O_2 = 8$) at $T_{in} = 25^\circ$C.

of the feed gases and the product gases could be reproduced in good agreement with the experimental observations.

Finally, we find a very good match between the simulations and the experimental results for diluted reaction mixtures (as shown in Fig. 7), while lower dilution, corresponding to higher reactor temperatures, yield increasing discrepancies between simulations

and experiment, with simulated selectivities and conversions being consistently higher than experimental ones. This seems to confirm the assumption that at the very high reaction temperatures that characterise the current reaction system a blind activity of the reactor steel (which is not accounted for in the model) leads to a deterioration of the reactor performance.

Overall, the countercurrent reactor concept with integrated heat exchange fulfils the expectations based on the analysis of the original reactor model. From a practical point of view, some hurdles still remain to be taken, among them primarily the question of a non-catalytic, high temperature-resistant reactor material that could replace the stainless steel used in our laboratory reactor. Nevertheless, the reactor concept is simple, safe and effective and thus seems very promising.

4.2. Distributed oxygen feed

The second conclusion drawn from the analysis of the reaction mechanism was based on the observation that a strong total oxidation pulse exists near the reactor entrance due to the high sticking coefficient of oxygen. This leads to an over-stoichiometric oxygen supply on the catalyst surface and thus deteriorates the reaction selectivities. Therefore, it seems a logical conclusion to distribute the oxygen supply to the reaction zone, reducing the local oxygen partial pressure and thus the oxygen flux to the catalyst surface. This can be realised for example in a membrane reactor, in which the membrane serves to selectively feed one of the reactants to the reaction system. An additional advantage of this reactor configuration would be that the hydrocarbon and the oxygen would not have to be pre-mixed outside the reaction zone, thus completely avoiding the danger of explosions.

So far, we analysed the possibilities of this reactor concept only in simulation studies. The above presented model was modified to allowed for different oxygen feed distributions along the reactor axis. Two representative results are shown in Fig. 8 in comparison with results for a conventional fixed bed reactor without feed distribution. In the first example the oxy-

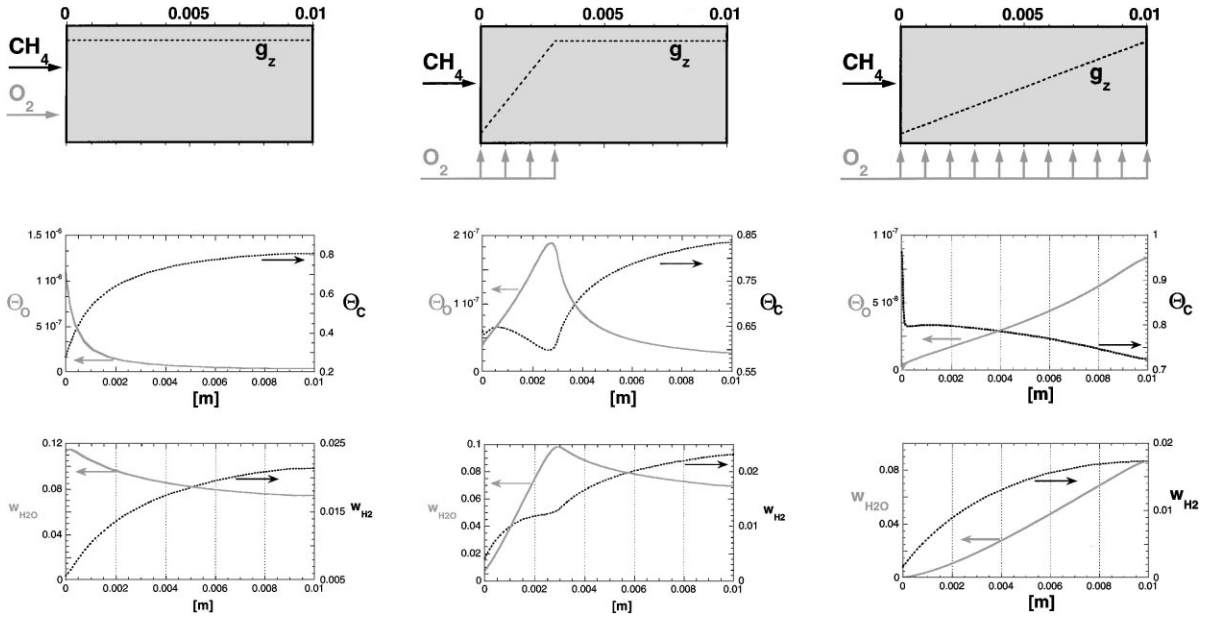

Fig. 8. Simulation results for methane oxidation with air over Pt in a catalytic membrane reactor with oxygen feed distribution: conventional fixed bed reactor (left-hand side column) in comparison with oxygen feed distribution over one-third of the reactor length (middle column) and over the whole length of the reactor (right-hand side column). A schematic picture of the reactor feed and resulting mass flow density, g_z, (top row), oxygen and carbon coverage profiles (middle row), and H_2 and H_2O mass fractions (bottom row) along the reactor axis at steady state. Conditions were: $CH_4/O_2 = 1.6$, $N_2/O_2 = 4$, $T = 1300^{\circ}C$ (isothermal), and $\dot{V}_{\text{in, total}} = 3$ slpm.

gen feed was distributed over one-third of the reactor length (shown in column 2 in Fig. 8) and in the second example, the oxygen feed was distributed equally over the whole reactor length (column 3). while the results shown are taken from isothermal simulations, simulation with energy balance show qualitatively the same behaviour and are not discussed here due to space limitations.

Clearly, the feed distribution allows to effectively tailor the coverage and concentration profiles along the reactor axis. The carbon and oxygen coverages are even completely inverted from their profiles in the conventional fixed bed reactor: in the latter, a small but pronounced oxygen coverage peak existed at the reactor entrance, behind which a very high carbon coverage was built up gradually. In sharp contrast to that, the reactor with equal oxygen feed distribution shows a strong peak in the carbon coverage at the reactor entrance, behind which the oxygen coverage builds up slowly. As apparent from the "intermediate" case, where the oxygen feed was distributed over the first third of the reactor, a maximum in the oxygen coverage and a corresponding minimum in the carbon coverage develops at the end point of the oxygen feed.

However, the concentration profiles reveal a problem of this reactor configuration (see Fig. 8, bottom row): despite the effective tailoring of the coverage profiles and the feed concentrations (not shown in the figure), the concentration profiles of H_2 and H_2O only reflect these changes very weakly. Calculated conversions and selectivities even *decrease* with increasing oxygen distribution (from a methane conversion of 78% at an H_2 selectivity of 72% for the conventional reactor to 71% conversion at 64% selectivity for oxygen feed distribution over the whole reactor length). This can be traced back to the very high reactivity of the partial oxidation products H_2 and CO: the decreased oxygen partial pressure (and correspondingly decreased oxygen coverage on the catalyst surface) initially lead to a strong increase in the syngas selectivities (as apparent from the decreasing H_2O mass fractions with increasing degree of oxygen distribution in Fig. 8). This improvement, however, is countered by subsequent reactions of those partial oxidation products that were formed in the initial parts of the reactor with the oxygen feed in the later part of the reactor. Thus, due to considerably higher reactivity of the syngas components compared to methane, the beneficial effect of suppressing the total oxidation zone at the reactor entrance is annihilated by sequential reactions in the latter part of the reactor. Clearly, a more detailed optimisation is needed to identify conditions, under which the strong influence of the distributed feed upon the catalyst coverages can be effectively put to work. One such reactor configuration could be an additional membrane (such as a Pd membrane) through which the highly reactive H_2 could be selectively removed before further reactions could occur.

While these first simulation results indicate that the *principle* behind the reactor concept works, important hurdles have to be taken before realising the concept in a working reactor. In addition to the problem of the high reactivity of the desired reaction products, particularly the question of high temperature resistant membrane materials and their sealing to standard steel tubing remains a central problem at this point [11,12]. Thus, while it seems that this concept holds interesting potential, much more work needs to be done both on the reaction engineering as well as on the material development before a truly successful realisation of a membrane reactor for the partial oxidation of methane will become a viable concept for industrial applications.

5. Summary and conclusions

We presented results from a detailed simulation study which allowed further insights into the reaction mechanism of catalytic methane oxidation over platinum catalysts. The results demonstrate that the reaction system is dominated by the transition from an oxygen covered surface at ignition to a strongly carbon covered surface under reaction conditions. This transition is accompanied by a switch of the primary reaction pathway from total to partial oxidation. Corresponding to this temporal development during ignition, the spatial reactor profiles under steady state conditions show a small oxygen covered zone near the reactor entrance in which the surplus of surface oxygen leads to total oxidation of the reactants and thus to a noticeable loss in reaction selectivity. Behind this zone, a high carbon coverage builds up on the catalyst surface, and the reaction switches to very selective syngas formation. Furthermore, the simulations showed that very high reaction tempera-

tures are essential for best reaction selectivities and conversions.

Based on these insights into the reaction mechanism and the reaction progress along the reactor axis, two new integrated reactor concepts were suggested, which seem promising alternatives to current monolith reactors. Both reactor safety as well as reaction conversions and selectivities were used as design guidelines.

Countercurrent heat-exchange reactor: High reaction and feed temperatures can be reached in a very cost efficient way through an effective heat integration into the reactor. This was achieved through thermal coupling of the feed gases with the effluent gases in a countercurrent heat-exchange reactor. Thus, very high reaction temperatures were reached, substantially increasing reaction selectivities and conversions. The effectiveness of this reactor concept could be shown both in simulation studies and in an experimental realisation of the reactor concept.

Catalytic membrane reactor: The build-up of a high oxygen coverage in the reactor entrance zone can be avoided by reducing the local oxygen partial pressure in this area. This can be achieved through a distributed oxygen feed along the reactor length such as in a catalytic membrane reactor. While simulations showed that this allows a very effective tailoring of surface coverages and a suppression of the total oxidation zone near the reactor entrance, no effective increase in reaction selectivities could be achieved so far due to the high reactivity of the partial oxidation products. Furthermore, several hurdles still remain to be taken on the way to an experimental realisation of this reactor concept.

Finally, a logical synthesis between the two presented reactor concepts could be seen in a reverse flow reactor concept (RFR), in which the periodic flow reversal in the reactor could combine the two above mentioned advantages: the feed gases entering the reactor would first encounter a strongly carbon covered catalyst surface, which should suppress the built-up of a high oxygen coverage at either reactor end. At the same time, the well known effective heat integration in a reverse-flow reactor [13] would again allow to raise the reaction temperatures and thus increase selectivites and conversions. However, due to its inherent transient operation, this reactor concept also shows the highest degree of complexity among the suggested configurations. Detailed studies of the reactor dynamics are therefore needed and are currently under way to evaluate the potential of this configuration.

Acknowledgements

Financial support by the Deutsche Forschungsgemeinschaft (DFG) is gratefully acknowledged.

References

[1] J. Frauhammer, G. Veser, Elementarkinetische Modellierung der katalytischen Oxiation von Methan zu Synthesegas in einem Monolithreaktor, Chem. Ing. Tech. 70 (1998) 1020–1026.
[2] D.A. Hickman, L.D. Schmidt, Syngas formation by direct oxidation of methane, Science 259 (1993) 343–346.
[3] Y.K. Park, D.G. Vlachos, Kinetically driven instabilities and selectivities in methane oxidation, AIChE J. 43 (1997) 2083–2095.
[4] G. Veser, J. Frauhammer, L.D. Schmidt, G. Eigenberger, Catalytic ignition during methane oxidation on platinum. experiments and modeling, in: G.F. Froment, K.C. Waugh (Eds.), Dynamics of Surfaces and Reaction Kinetics in Heterogeneous Catalysis, Stud. Surf. Sci. Catal. Vol. 109, Elsevier, Amsterdam, 1997, p. 273–284.
[5] D.A. Hickman, L.D. Schmidt, Syngas production by direct oxidation of methane on monoliths, J. Catal. 138 (1992) 267–282.
[6] G. Veser, J. Frauhammer, Modeling steady state ignition during catalytic methane oxidation in a monolith reactor, Chem. Eng. Sci. 55 (2000) 2271–2286.
[7] U. Nowak, J. Frauhammer, U. Nieken, A fully adaptive algorithm for parabolic differential equations in one space dimension, Comput. Chem. Eng. 20 (1996) 547–561.
[8] D.J. Hucknall, The Chemisty of Hydrocarbon Combustion, Chapman & Hall, London, 1985.
[9] C.T. Bowman, R.K. Hanson, D.F. Davidson, W.C. Gardiner, V. Lissianski, G.P. Smith, D.M. Golden, M. Frenklach, M. Goldenberg, GRI-Mech 2.11. http://www.me.berkeley.edu/gri_mech/.
[10] U. Friedle, G. Veser, A counter-current heat-exchange reactor for high-temperature partial oxidation reactions, Chem. Eng. Sci. 54 (1999) 1325–1332.
[11] G. Kolios, G. Veser, G. Eigenberger, Catalytic membrane reactors for selective oxidation reactions, in: Proceedings of the Fourth ESF Workshop on Membrane Reactors, Oslo, 1997.
[12] G. Saracco, G.F. Versteeg, W.P.M. van Swaaij, Current hurdles to the success of high-temperature membrane reactors, J. Memb. Sci. 95 (1984) 105–123.
[13] G. Eigenberger, U. Nieken, Catalytic combustion with periodic flow reversal, Chem. Eng. Sci. 42 (1988) 2109–2115.